Infrared and Raman Spectra, Conformational Stability, *ab Initio* Calculations, and Vibrational Assignments for Cyclopropylchlorosilane

T. K. Gounev, Jeffery W. Weston, and Shiyu Shen

Department of Chemistry, University of Missouri−Kansas City, Kansas City, Missouri 64110-2499

M. Dakkouri and A. Grunvogel-Hurst

Abterlung für Physikalische, Chemie Universität Ulm, 7900 Ulm, Germany

J. R. Durig*

Department of Geosciences, University of Missouri−Kansas City, Kansas City, Missouri 64110-2499

Received: June 10, 1997; In Final Form: August 14, 1997[⊗]

The infrared (3300−30 cm^{-1}) spectra of gaseous and solid cyclopropylchlorosilane, c-$C_3H_5SiH_2Cl$, have been recorded. Additionally, the Raman spectra (3200−30 cm^{-1}) of the liquid and solid have been recorded and quantitative depolarization values obtained. Both the cis and gauche conformers have been identified in the fluid phases but only the gauche conformer remains in the solid. Variable-temperature (−55 to −100 °C) studies of the infrared spectra of the sample dissolved in liquid xenon have been carried out. From these data, the enthalpy difference has been determined to be 98 ± 10 cm^{-1} (280 ± 29 cal mol^{-1}), but with the cis conformer being the more stable form which is consistent with the predictions from *ab initio* calculations at the highest level of calculation, MP2/6-311++G**. A complete vibrational assignment is proposed for both the cis and gauche conformers based on infrared band contours, relative intensities, depolarization values, and group frequencies. The vibrational assignments are supported by normal-coordinate calculations utilizing the force constants from *ab initio* MP2/6-31G* calculations. Complete equilibrium geometries have been determined for both rotamers by *ab initio* calculations employing a variety of basis sets up to 6-311++G** at levels of restricted Hartree−Fock (RHF) and/or Moller−Plesset (MP) to second order. The potential energy terms for the conformer interconversion have been obtained from the MP2/6-31G* calculation. The results are discussed and compared to those obtained for some similar molecules.

Introduction

Three-membered ring molecules substituted with an asymmetric internal rotor are of interest to structural chemists because of the possibility of the presence of conformers at ambient temperature. For the halomethylcyclopropanes, c-$C_3H_5CH_2X$, where X = F, Cl, Br, and I, there was considerable controversy as to whether more than one conformer was present at room temperature. Fluoromethylcyclopropane is so unstable that only theoretical predictions are available on its conformational stability.[1] For chloromethylcyclopropane, Fujiwara et al.[2] from a microwave study proposed that the molecule exists as a conformational equilibrium between the gauche and cis rotamers at ambient temperature. However, Mohammadi and Brooks,[3,4] also from an investigation of the microwave spectrum, concluded that only the gauche conformer is present in the gas where they found no evidence for the cis rotamer. From molecular mechanics calculations used in conjunction with electron diffraction experiments it was concluded[5] that the gauche conformer is the predominant form with the energy difference between the conformers predicted from these calculations to be 577 cm^{-1} (1.65 kcal/mol). This value is about twice the ΔH value of 273 ± 108 cm^{-1} (728 ± 309 cal/mol) obtained from a variable temperature Raman study of the gas where clearly the gauche conformer was shown to be the more stable form.[6] Kalasinsky and Wurrey[7] from the vibrational and ΔH studies have concluded that the relative abundances of the isomers of chloromethylcyclopropane are 95% gauche and 5% cis in the liquid phase at room temperature. Further studies on the corresponding bromide and iodide molecules indicate that as the halogen atom increases in size the amount of the cis conformer decreases.[7−11]

These experimental results are consistent with some recent predictions from molecular mechanics calculations where fluoromethylcyclopropane is proposed to have the cis rotamer the most stable form whereas all the other halomethylcyclopropane molecules should have the gauche conformers the most stable forms.[11] In contrast, the corresponding silyl molecules, c-$C_3H_5SiH_2X$, where X = F, Cl, Br, and I, are predicted to have the cis conformer as the most stable form.[11] These predictions, however, are not supported by any experimental results, and the proposed conformational behavior of halosilylcyclopropanes needs verification. Therefore, we have undertaken a conformational study of cyclopropylchlorosilane utilizing vibrational spectroscopy.

We have recorded the infrared and Raman spectra of the fluid and solid phases of cyclopropylchlorosilane and proposed a complete vibrational assignment. Additionally, we have recorded variable-temperature studies of the infrared spectra of the sample dissolved in liquid xenon. We have also carried out *ab initio* calculations employing a variety of basis sets up to 6-311++G** at levels of restricted Hartree−Fock (RHF) and Moller−Plesset (MP) to second order to obtain complete equilibrium geometries. The force constants, vibrational frequencies, infrared and Raman intensities, and conformational stabilities have also been obtained from the *ab initio* calculations.

* Corresponding author.

[⊗] Abstract published in *Advance ACS Abstracts,* October 15, 1997.

S1089-5639(97)01894-X CCC: $14.00 © 1997 American Chemical Society

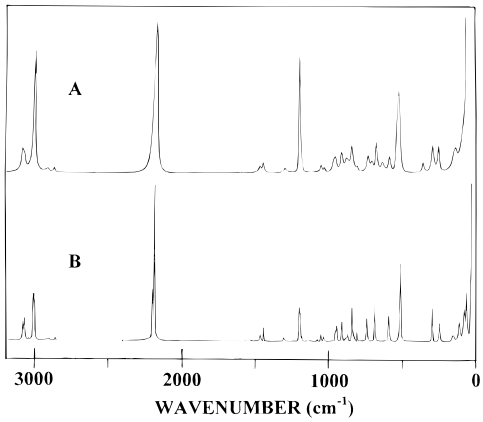

Figure 1. Raman spectra of cyclopropylchlorosilane in the (A) liquid; and (B) annealed solid.

The results of these vibrational spectroscopic and theoretical studies are reported herein.

Experimental Section

The preparation of cyclopropylchlorosilane was carried out according to the following reactions which will be described in more detail elsewhere.[12] The starting material, vinyltrimethoxysilane, was prepared as described previously.[13] The cyclopropanation reaction to trimethoxysilylcyclopropane was carried out using a slightly modified Simons−Smtih procedure.[14] This modification incorporated mainly the application of the sonication technique (Bronson equipment, 50 Hz, 250 W). The utilization of ultrasound irradiation provided two significant advantages: promotion of the reaction leading to higher yields and the use of only Zn instead of the commonly utilized Zn−Cu mixture. A stirred slurry of Zn and vinyltrimethoxysilane in hexane was sonicated and simultaneously methylene iodide was added. After the solvent was evaporated, purification was carried out with a spinning band column which gave trimethoxysilylcyclopropane, bp 68−70 °C/37.5 Torr. The treatment of trimethoxysilylcyclopropane with $LiAlH_4$ led to cyclopropylsilane.[15] The chlorination of cyclopropylsilane to cyclopropylmonochlosilane was achieved by the dropwise addition (at about 5 °C) of equivalent amount (1:1 mol) of anhydrous freshly distilled $SnCl_4$ to a solution of cyclopropylsilane in *n*-butyl ether. The crude product was initially purified with a spinning band column under anhydrous conditions which gives moderately pure cyclopropylchlorosilane, bp 73.8−74.0 °C/688 Torr. Further purification was carried out on a low-temperature, low-pressure fractionization column, and the purity of the sample was checked by mass spectrometry and the expected mid-infrared spectrum of the gas based on the predicted spectrum from *ab initio* calculations. The sample was stored in the dark under vacuum in a sample tube with a greaseless stopcock and held at dry ice temperature until used. All sample transfers were carried out under vacuum to avoid contamination.

The Raman spectra of cyclopropylchlorosilane from 3200 to 20 cm^{-1} (Figure 1) were recorded on a SPEX Model 1403 spectrophotometer equipped with a Spectra-Physics Model 164 argon ion laser operating on the 5145 Å line. Laser power at the sample ranged from 0.4 to 1 W depending on the physical state of the sample. The spectrum of the liquid was obtained from the sample sealed in a glass capillary with a spherical bulb on the end.[16] The spectrum of the solid was obtained by condensing the liquid in a Miller−Harney cell[17] cooled by boiling liquid nitrogen. Multiple annealings were carried out to obtain good polycrystalline material which was indicated when no further changes in the spectrum were noted. The reported frequencies are expected to be accurate to ±2 cm^{-1}.

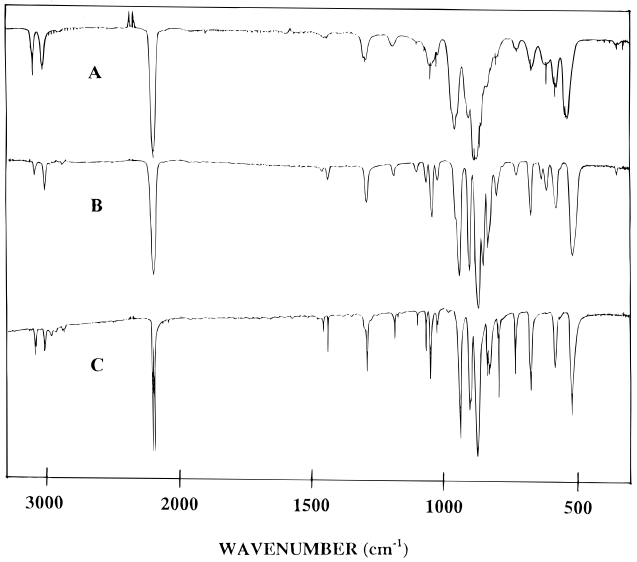

Figure 2. Mid-infrared spectra of cyclopropylchlorosilane in the (A) gas, (B) unannealed solid, and (C) annealed solid.

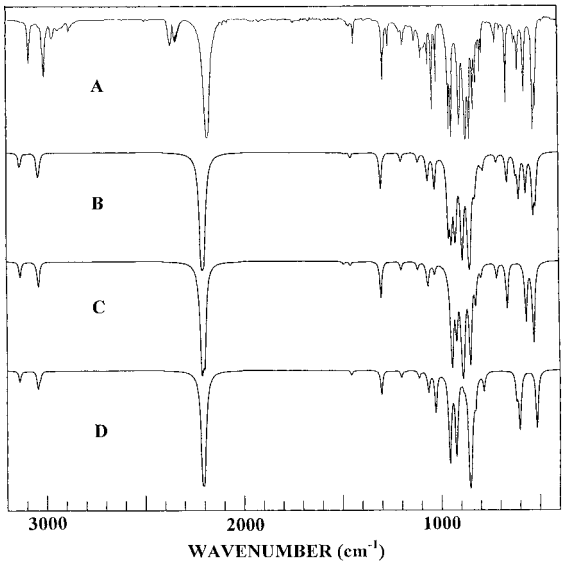

Figure 3. Mid-infrared spectra of cyclopropylchlorosilane: (A) xenon solution at −70 °C; (B) calculated spectrum of the mixture of both conformers; (C) calculated spectrum of the gauche conformer; and (D) calculated spectrum of the cis conformer.

The mid-infrared spectra of gaseous and solid cyclopropylchlorosilane (Figure 2) were recorded on a Perkin-Elmer Model 2000 Fourier transform interferometer equipped with a ceramic source, Ge/CsI beam splitter, and a DTGS detector. A 10 cm cell with CsI windows was used to obtain the spectrum of the gas. The spectrum of the solid was obtained by condensing the sample on a CsI substrate held at 77 K by boiling liquid nitrogen. The sample was repeatedly annealed until no further changes were observed in the spectra.

The mid-infrared spectra of the sample dissolved in liquified xenon (Figure 3A) were recorded on a Bruker Model IFS-66 Fourier transform interferometer equipped with a Globar source, Ge/KBr beam splitter, and a DTGS detector. The spectra were recorded at variable temperatures ranging from −55 to −100 °C with 100 scans at a resolution of 1.0 cm^{-1}. The temperature studies in the liquified noble gas were carried out in a specially designed cryostat cell which is composed of a copper cell with a 4 cm path length and wedged silicon windows sealed to the

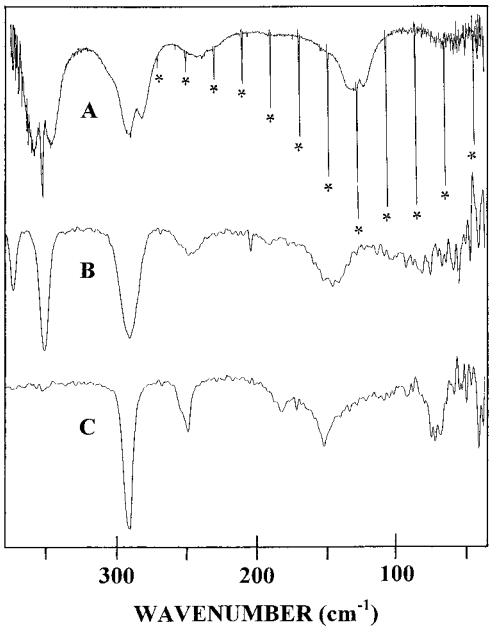

Figure 4. Far-infrared spectra of cyclopropylchlorosilane in the (A) gas, (B) unannealed solid, and (C) annealed solid. The bands labeled with an asterisk are due to the rotational transitions of HCl.

cell with indium gaskets. The temperature is monitored by two Pt thermoresistors and the cell is cooled by boiling liquid nitrogen. The complete cell is connected to a pressure manifold to allow for the filling and evacuation of the cell. After the cell is cooled to the desired temperature, a small amount of sample is condensed into the cell. Next, the pressure manifold and the cell are pressurized with xenon, which immediately starts condensing in the cell, allowing the compound to dissolve.

The far-infrared spectrum of the gas (Figure 4A) was recorded on a Bomem Model DA3.002 Fourier transform interferometer equipped with a vacuum bench, a Globar source, and a liquid He cooled silicon bolometer with a wedged sapphire filter and polyethylene windows. The gaseous sample was contained in a 1 m cell equipped with polyethylene windows and recorded at a spectral resolution of 0.2 cm^{-1} with a 6.25 μm Mylar beam splitter. The far-infrared spectra of the solid (Figure 4, B and C) were recorded on the previously described Perkin-Elmer Model 2000 interferometer. A grid beam splitter and a cryostat cell with polyethylene windows were used and the sample was deposited on a silicon substrate at −196 °C. All observed infrared and Raman bands with significant intensities are listed in Table 1.

Ab Initio Calculations

The LCAO-MO-SCF restricted Hartree−Fock calculations were performed with the Gaussian-92 program[18] using Gaussian-type basis functions. The energy minima with respect to nuclear coordinates were obtained by the simultaneous relaxation of all of the geometric parameters using the gradient method of Pulay.[19] The structural optimizations for both the cis and the gauche conformers were carried out with initial parameters taken from those of cyclopropyldichlorosilane.[20] The 6-31G*, 6-31G**, 6-311G**, 6-31++G**, 6-311+G**, and 6-311++G** basis sets were employed at the level of restricted Hartree−Fock (RHF) and Moller−Plesset (MP2) to second order. The determined structural parameters are listed in Table 2.

The *ab initio* MP2/6-31G* calculations were utilized to obtain theoretical vibrational force constants for both the cis and the gauche conformers of cyclopropylchlorosilane, and the resulting wavenumbers were used for comparison with the experimental results. To obtain the approximate descriptions of the normal modes it was necessary to transform the *ab initio* force fields in terms of Cartesian coordinates into force fields in terms of the more convenient internal coordinates. The corresponding transformation matrices, **B**, were generated by using the Cartesian coordinates obtained for the optimized geometries and the complete set of 34 internal coordinates shown in Figure 5. This complete set of internal coordinates was used to form the symmetry coordinates listed in Table 3. The resulting force fields in internal coordinates for the cis and gauche conformers, which can be obtained from the authors, were input along with the unsymmetrized **G** matrices and scaling factors, in the perturbation program written by Schachtschneider.[21] Initially, all scaling factors were kept fixed at a value of 1.0 to produce the pure *ab initio* calculated vibrational frequencies. Scaling factors of 0.9 for the stretching and bending coordinates and 1.0 for torsions were used to obtain the "fixed scaled" force fields and vibrational wavenumbers along with the potential energy distributions (PED). All of these data are listed in Table 4 for the cis and gauche conformers.

Conformational Stability

There are several fundamentals which show conformer doublets in both the infrared and Raman spectra of the fluid phases. The two bands at 668 and 628 cm^{-1} in the Raman spectrum of the liquid are assigned to the Si−C stretching modes, but in the spectra of the solid only the higher frequency band remains. Similarly, the two Q-branches at 610 and 578 cm^{-1} in the infrared spectrum of the gas are assigned as SiH_2 rocks, but this time only the lower frequency band remains in the spectrum of the solid. Other bands which are observed in the spectra of the fluid phases but not present in the spectrum of the annealed solid are found at 960, 855, 829, 788, 697, and 351 cm^{-1}. These data clearly show that there are two conformers present in the fluid phases at ambient temperatures but only one rotamer remains in the polycrystalline solid. The band at 351 cm^{-1} is the only one predicted by the *ab initio* calculations in the 300 cm^{-1} region and is definitely assigned to the ring−Si bend of the cis conformer. Since this band disappears from the spectrum of the solid, it can be concluded that only the gauche conformer remains in the annealed solid. Further support for this conclusion is found from the assignments for the C−Si stretch and SiH_2 rock which are assigned at 629 and 610 cm^{-1} for the cis conformer in the amorphous solid and at 671 and 576 cm^{-1}, respectively, for the gauche rotamer. Only the latter two bands remain in the spectrum of the polycrystalline solid. Similarly, the other listed bands which disappear upon solidification and annealing are all assigned as arising from the cis conformer as will be discussed later. Therefore, all the spectral data indicate that the gauche form is the stable conformer in the annealed solid.

In order to gain information about the enthalpy difference between the two conformers a variable temperature study in liquified xenon was carried out. The sample was dissolved in the liquified xenon and the spectra were recorded at different temperatures varying from −55 to −100 °C. Only small interactions are expected to occur between the dissolved sample and the surrounding xenon atoms and, consequently, only small frequency shifts are anticipated when passing from the gas phase to the liquified noble gas solutions.[22−24] Thus, the resulting spectrum (Figure 3A) should be representative of the infrared spectrum of the vapor phase without the band broadening rotational branches. A significant advantage of this type of temperature study is that the conformer bands are better resolved in comparison with those in the infrared spectrum of the gas

TABLE 1: Observed[a] Infrared and Raman Wavenumbers (cm^{-1}) for Cyclopropylchlorosilane

infrared						Raman					assignment
gas	rel. int	xenon solution	rel int	solid	rel int	liquid	rel. int/depol	solid	rel int	ν_i[b]	approximate description
3095 R											
3091 Q,A	m	3079	m	3078	w	3082	w,dp	3079	w	ν_1, ν_1'	CH_2 antisymmetric stretch
3089 Q,A	m			3067	w	3073	w,dp	3068	w	ν_{18}, ν_{18}'	CH_2 antisymmetric stretch
3084 P											
								3040	vw		$\nu_4' + \nu_{12}'$
		3029	w					3026	vw		$\nu_4' + \nu_{25}'$
3018 R				3014	vw						
3014 Q	m	3003	m	3007	w	3007	s,p	3009	m	ν_2, ν_2', ν_3, ν_3'	CH stretch, CH_2 symmetric stretch
3009				3000	w			3001	m	ν_{19}, ν_{19}'	CH_2 symmetric stretch
		2962	vw	2952	vw	2942	vw,p				
				2911	vw	2911	vw,p				$\nu_4' + \nu_{27}'$
2885	vw,bd	2878	vw								$\nu_4 + \nu_{27}$
		2865	vw	2861	vw	2867	vw,p	2859	vw		$\nu_4' + \nu_{14}'$
2216 Q,C	vw										impurity
2193 R				2196	vs						
2189 Q	vs	2180	vs,bd	2192	s,sh			2197	s	ν_{20}, ν_{20}'	SiH_2 antisymmetric stretch
2186 Q	vs									ν_4	SiH_2 symmetric stretch
2185 Q	vs			2180	vs	2178	vs,p	2185	vvs	ν_4'	SiH_2 symmetric stretch
2180 P											
1457 Q	vw	1457	vw	1451	vw	1460	w,p	1458	w	ν_5, ν_5'	CH_2 deformation
1436 Q	vw	1436	w	1434	w			1435	w	ν_{21}'	CH_2 deformation
		1430	w			1438	w,dp			ν_{21}	CH_2 deformation
1297 R											
1293 Q	w	1289	m							ν_6	CH bend (in-plane)
				1293	sh,vw			1296	vw		
1292 Q,A	w	1281	sh,w	1285	m	1289	vw,p	1289	sh,vw	ν_6'	CH bend (in-plane)
1287 P											
1190 Q	vw	1188	w							ν_7	ring breathing
1186 Q	vw	1183	w			1189	s,p	1190	m	ν_7'	ring breathing
				1181	w			1184	sh,m		
1178 Q,C	vw	1175	vw	1169	vw			1172	vw	ν_{22}, ν_{22}'	CH_2 twist
		1127	w								impurity
1096 Q	vw	1095	w	1096	vw					ν_{23}'	CH bend (out-of-plane)
1095 Q	vw									ν_{23}	CH bend (out-of-plane)
1068 Q,C	vw	1062	sh,vw							ν_{24}	CH_2 wag
1064 Q	vw	1060	w	1065	w	1066	vw,dp	1067	vw	ν_{24}'	CH_2 wag
				1063	w						
1049 R											
1045 Q,A	m	1041	s	1048	m	1043	w,p	1043	w	ν_8, ν_8'	CH_2 wag
1040 P											
1026 R											
1022 Q,A	w	1019	m	1023	vw	1021	w,p	1024	vw	ν_9, ν_9'	CH_2 twist
1016 P				1018	vw						
964 R											
960 Q	s	956	s			956	sh,w,p			ν_{10}	SiH_2 deformation
954 R											
946 crt,B	s	943	vs			945	w,dp	945	w	ν_{10}'	SiH_2 deformation
942 P				935	s			936	w		
911 R											
906 Q	s	904	s							ν_{11}	ring deformation
901 P		899	sh,s	900	s	903	w,p	900	w	ν_{11}'	ring deformation
				894	sh,m						
885 R											
879 Q,A	vs	873	vs	871	vs	869	w,dp	870	vw	ν_{12}', ν_{25}	SiH_2 wag, ring deformation
								860	vw		
873 P											
860 Q,A	vs	854	vs			855	sh,w,p			ν_{12}	SiH_2 wag
854 R											
845 R											
840 Q	m	834	s	834	m	833	w,dp	832	m	ν_{25}'	ring deformation
835 P											
829 Q	w	823	sh,m							ν_{26}	CH_2 rock
				827	m						
824 Q	w	819	m	822	w			823	sh,vw	ν_{26}'	CH_2 rock
819 P											
802 R											
798 Q,A	w	796	m	797	vw	800	w,p	798	w	ν_{13}'	CH_2 rock
794 P				795	vw						
				790	m						
788 Q	vw	787	w							ν_{13}	
725 R											CH_2 rock
721 Q,A	vw	721	w	727	m	723	w,p	731	m	ν_{27}'	SiH_2 twist

TABLE 1 (Continued)

infrared						Raman					assignment
gas	rel. int	xenon solution	rel int	solid	rel int	liquid	rel. int/depol	solid	rel int	ν_i[b]	approximate description
716 P											
		698	vw			697	w,dp			ν_{27}	SiH_2 twist
673 R											
669 Q	w	667	s	675	sh,w	668	w,p	678	m	ν_{14}'	CSi stretch
666 Q	w			670	m						
662 P											
		626	w			628	w,p			ν_{14}	CSi stretch
615 R											
610 Q,C	m	608	m							ν_{28}	SiH_2 rock
605 P											
583 R				581	w						
578 Q,A	m	577	m	575	sh,w	578	w,p	583	m	ν_{28}'	SiH_2 rock
573 P											
543 R											
539 Q,A	s	531	s	518	s	530	sh,w,p	503	s	ν_{15}'	SiCl stretch
		525	sh,s								
533 max	s	519	s			515	m,p			ν_{15}	SiCl stretch
		513	sh,m								
354 R											
349 Q,A	vw					351	w,p			ν_{16}	ring−Si bend (in-plane)
343 P											
288 R											
283 ctr,B	vw			291	m	287	w,p	289	m	ν_{29}'	ring−Si bend (out-of-plane)
278 P											
235 ctr	vw			249	w	248	w,p	239	w	ν_{16}'	ring−Si bend (in-plane)
				181	vw						
128 R											
124 crt,B	vw			151	w	135	w,p	149	vw	ν_{17}, ν_{17}'	CSiCl bend
120 P											
68 Q	vw									ν_{30}	$SiClH_2$ torsion
64 Q	vw										
57 Q	vw									ν_{30}'	$SiClH_2$ torsion
55 Q	vw										
								107	w		
				73	w			75	m		
								61	m		lattice modes
				40	w			32	w		

[a] Abbreviations used: s, strong, m, moderate; w, weak; v, very; bd, broad; sh, shoulder; p, polarized; dp, depolarized; A, B, and C refer to infrared band envelopes; P, Q, and R refer to the rotational−vibrational branches. [b] ν_i and ν_i' refer to the assignments made for the cis and gauche conformers, respectively.

(Figure 2A). This is particularly important since most of the conformer bands for this molecule are expected to be observed within a few wavenumbers of each other.

The best separated conformer bands in the infrared spectra of the xenon solutions are those assigned to the C−Si stretches and SiH_2 rocks (Figure 6) as indicated earlier. Additionally well suited for variable-temperature measurements are the conformer pairs for the CH_2 rock and SiH_2 deformation. The relative intensity of the above-mentioned four fundamentals of the cis and gauche conformers were measured as a function of temperature and their ratios were determined. Ten sets of spectral data were obtained for these four pairs of conformer bands. By application of the van't Hoff equation $-1n\ K = (\Delta H/RT) - (\Delta S/R)$, where ΔS is the entropy change, we have determined ΔH from a plot of $-1n\ K$ versus $1/T$, where $\Delta H/R$ is the slope of the line and K is the appropriate intensity ratio. It is assumed that ΔH is not a function of temperature. Each conformer pair leads to a ΔH value and an uncertainty associated with it (Table 5). The combined fit of all data is consistent with an enthalpy difference of 98 ± 10 cm^{-1} (281 ± 29 cal/mol) with the cis conformer being more stable. The error limits are given by the standard deviation of the measured areas of the intensity data, which does not take into account small associations with the liquid xenon or other experimental factors such as underlying overtone or combination bands. Thus, the cis conformer is the more stable rotamer in the gas and the gauche conformer is the only form in the annealed solid.

Vibrational Assignment

The conformational analysis of cyclopropylchlorosilane shows that the molecule exists in two stable conformations. The cis conformer has a plane of symmetry and its 30 normal modes are classified by the symmetry species of the C_s symmetry group (A′ and A″). The 17 A′ modes should produce polarized Raman bands and A/B-type infrared band contours, whereas the 13 A″ modes should be depolarized in the Raman spectra and give rise to C-type band envelopes. The *gauche* conformer has only the trivial C_1 symmetry and all 30 vibrations should yield polarized Raman bands and hybrid A/B/C-type infrared band contours. Guided by these considerations and also by the calculated spectral intensities and normal-coordinate analysis, we proposed the assignment of the infrared and Raman spectra of c-$C_3H_5SiH_2Cl$ given in Table 1.

The assignments of the carbon−hydrogen modes have been previously reported for cyclopropyldichlorosilane,[20] and with only minor frequency shifts, they remain essentially the same for cyclopropylchlorosilane. In fact, the spectra of these two compounds look remarkably similar down to about 1000 cm^{-1}. The SiH_2 stretches give rise to a very strong and polarized band in the Raman spectrum of the liquid which splits into two bands, one at 2197 cm^{-1} for the antisymmetric stretch and another at 2185 cm^{-1} for the symmetric stretch. The Q-branch at 2216 cm^{-1} in the infrared spectrum of the gas is due to an impurity from cyclopropyldichlorosilane.[20]

TABLE 2: Structural Parameters,[a] Rotational Constants, Dipole Moments, and Total Energies for Cyclopropylchlorosilane

	RHF/6-31G*		MP2/6-31G**		MP2/6-311G**		MP2/6-31++G**		MP2/6-311+G**		MP2/6-311++G**	
parameter	cis	gauche	cis	gauche	cis	gauche	cis	gauche	cis	gauche	cis	gauche
$r(C_1-C_2)$	1.511	1.515	1.513	1.518	1.520	1.524	1.515	1.519	1.520	1.525	1.520	1.525
$r(C_1-C_3)$	1.511	1.509	1.513	1.513	1.520	1.519	1.515	1.515	1.520	1.520	1.520	1.520
$r(C_1-S_i)$	1.858	1.854	1.849	1.843	1.845	1.839	1.850	1.844	1.845	1.840	1.846	1.840
r(Si−Cl)	2.079	2.078	2.065	2.065	2.064	2.064	2.067	2.066	2.066	2.065	2.067	2.065
$r(C_1-H_6)$	1.081	1.079	1.084	1.082	1.088	1.086	1.085	1.083	1.088	1.087	1.088	1.087
$r(C_2-H_7)$	1.076	1.076	1.079	1.079	1.084	1.083	1.080	1.080	1.083	1.083	1.084	1.083
$r(C_2-H_8)$	1.076	1.077	1.080	1.081	1.084	1.085	1.081	1.081	1.084	1.085	1.084	1.085
$r(C_3-H_9)$	1.076	1.075	1.079	1.079	1.084	1.083	1.080	1.080	1.083	1.083	1.084	1.083
$r(C_3-H_{10})$	1.076	1.077	1.080	1.081	1.084	1.085	1.081	1.081	1.084	1.085	1.084	1.085
$r(Si_3-H_{11})$	1.471	1.472	1.472	1.473	1.471	1.473	1.471	1.472	1.472	1.473	1.472	1.473
$r(Si_4H_{12})$	1.471	1.471	1.472	1.472	1.471	1.471	1.471	1.471	1.472	1.471	1.472	1.471
$\angle(C_3C_2C_1)$	60.5	60.8	60.5	60.7	60.5	60.7	60.4	60.6	60.4	60.7	60.4	60.7
$\angle(SiC_1C_2)$	123.2	119.6	121.4	118.2	121.5	118.1	121.8	119.0	121.4	118.7	121.4	118.7
$\angle(Si_4C_1C_3)$	123.2	121.1	121.4	119.5	121.5	119.5	121.8	119.6	121.4	119.3	121.4	119.2
$\angle(ClSiC_1)$	109.9	110.7	108.4	111.1	108.2	111.0	108.3	110.4	107.8	110.5	107.8	110.4
$\angle(H_6C_1C_2)$	114.6	114.9	114.8	115.2	114.7	115.0	114.7	115.1	114.6	114.9	114.6	115.0
$\angle(H_6C_1C_3)$	114.6	115.0	114.8	115.3	114.7	115.2	114.7	115.2	114.6	115.1	114.6	115.1
$\angle(H_6C_1Si)$	112.5	115.5	114.3	117.0	114.5	117.3	114.0	116.6	114.7	117.1	114.6	117.1
$\angle(H_7C_2C_1)$	117.1	117.2	117.2	117.2	117.0	116.9	117.2	117.1	117.0	116.9	117.0	116.9
$\angle(H_8C_2C_1)$	118.5	118.7	118.1	118.4	118.0	118.2	118.2	118.4	117.9	118.2	118.0	118.2
$\angle(H_9C_3C_1)$	117.1	117.2	117.2	117.2	117.0	117.0	117.2	117.2	117.0	117.0	117.0	117.0
$\angle(H_{10}C_3C_1)$	118.5	118.5	118.1	118.1	118.0	117.9	118.2	118.1	117.9	117.9	118.0	117.9
$\angle(H_{11}SiC_1)$	111.8	109.8	112.0	108.1	112.1	108.3	111.8	108.5	112.0	108.3	112.0	108.4
$\angle(H_{12}SiC_1)$	111.8	112.2	112.0	112.5	112.1	112.5	111.8	112.3	112.0	112.5	112.0	112.5
$\tau(ClSiC_1H_6)$	180.0	−63.2	180.0	−64.2	180.0	−63.1	180.0	−66.2	180.0	−65.2	180.0	−65.6
$\tau(H_7C_2C_3C_1)$	106.9	106.8	107.0	106.8	106.8	106.6	107.0	106.8	106.8	106.6	107.0	106.7
$\tau(H_8C_2C_3C_1)$	−108.7	−108.8	−108.3	−108.6	−108.3	−108.3	−108.5	−108.6	−108.2	−108.4	−108.3	−108.4
$\tau(H_9C_3C_2C_1)$	−106.9	−107.0	−107.0	−107.1	−106.8	−106.9	−107.0	−107.1	−106.8	−106.9	−107.0	−106.9
$\tau(H_{10}C_3C_2C_1)$	108.7	108.7	108.3	108.3	108.3	108.2	108.5	108.3	108.2	108.1	108.3	108.1
$\tau(H_{11}SiC_1H_6)$	−61.5	178.5	−61.6	177.6	−62.1	179.1	−61.7	175.9	−62.1	177.2	−62.2	176.9
$\tau(H_{12}SiC_1H_6)$	61.5	55.4	61.6	55.5	62.1	56.1	61.7	53.2	62.1	53.9	62.2	53.5
$\lvert\mu_a\rvert$	2.246	2.725	2.124	2.622	2.162	2.652	2.031	2.504	2.006	2.497	1.995	2.496
$\lvert\mu_b\rvert$	1.254	0.672	1.224	0.611	1.248	0.618	1.182	0.613	1.202	0.605	1.199	0.611
$\lvert\mu_c\rvert$	0.000	0.123	0.000	0.163	0.000	0.164	0.000	0.159	0.000	0.160	0.000	0.165
$\lvert\mu_t\rvert$	2.573	2.809	2.452	2.697	2.496	2.728	2.350	2.583	2.339	2.574	2.328	2.572
A	5.354	8.028	5.269	8.065	5.245	8.086	5.258	7.889	5.219	7.928	5.219	7.901
B	2.000	1.553	2.097	1.575	2.103	1.570	2.086	1.591	2.114	1.588	2.112	1.591
C	1.673	1.398	1.732	1.418	1.736	1.417	1.725	1.425	1.740	1.425	1.739	1.427
$-E$	866.1107379	866.1113785	866.7881715	866.7885499	867.0818662	867.082120	866.8021493	866.8022557	867.0881339	867.0881735	867.0893852	867.089310
ΔE (cm^{-1})	141		83		56		23		9			17
a_0 (Å)	4.04	4.06	4.05	4.05	4.07	4.06	4.04	4.05	4.04	4.06	4.03	4.06

[a] Bond distances in Å, bond angles in degrees, rotational constants in MHz, dipole moments in debye, and total energies in hartrees.

TABLE 3: Symmetry Coordinates[a] for Cyclopropylchlorosilane

species	description	symmetry coordinate[a]
A′	CH_2 antisymmetric stretch	$S_1 = r_3 - r_4 + r_5 - r_6$
	CH_2 symmetric stretch	$S_2 = r_3 + r_4 + r_5 + r_6$
	CH stretch	$S_3 = r_2$
	SiH_2 symmetric stretch	$S_4 = S_1 + S_2$
	CH_2 deformation	$S_5 = 4\rho_1 - \alpha_1 - \beta_1 - \phi_1 - \eta_1 + 4\rho_2 - \alpha_2 - \beta_2 - \phi_2 - \eta_2$
	CH bend (in-plane)	$S_6 = 2\gamma - \mu_1 - \mu_2$
	ring breathing	$S_7 = R_1 + R_2 + R_3$
	CH_2 wag	$S_8 = \alpha_1 - \beta_1 + \phi_1 - \eta_1 + \alpha_2 - \beta_2 + \phi_2 - \eta_2$
	CH_2 twist	$S_9 = \alpha_1 - \beta_1 - \phi_1 + \eta_1 + \alpha_2 - \beta_2 - \phi_2 + \eta_2$
	SiH_2 deformation	$S_{10} = 4\delta - \pi_1 - \pi_2 - \sigma_1 - \sigma_2$
	ring deformation	$s_{11} = 2R_1 - R_2 - R_3$
	SiH_2 wag	$S_{12} = \pi_1 + \pi_2 - \sigma_1 - \sigma_2$
	CH_2 rock	$S_{13} = \alpha_1 + \beta_1 - \phi_1 - \eta_1 + \alpha_2 + \beta_2 - \phi_2 - \eta_2$
	CSi stretch	$S_{14} = T$
	SiCl stretch	$S_{15} = r_1$
	ring−Si bend (in-plane)	$S_{16} = \epsilon_1 + \epsilon_2$
	CSiCl bend	$S_{17} = 5\theta - \pi_1 - \pi_2 - \sigma_1 - \sigma_2 - \delta$
A″	CH_2 antisymmetric stretch	$S_{18} = r_3 - r_4 - r_5 + r_6$
	CH_2 symmetric stretch	$S_{19} = r_3 + r_4 - r_5 - r_6$
	SiH_2 antisymmetric stretch	$S_{20} = S_1 - S_2$
	CH_2 deformation	$S_{21} = 4\rho_1 - \alpha_1 - \beta_1 - \phi_1 - \eta_1 - {}_4\rho_2 + \alpha_2 + \beta_2 + \phi_2 + \eta_2$
	CH_2 twist	$S_{22} = \alpha_1 - \beta_1 - \phi_1 + \eta_1 - \alpha_2 + \beta_2 + \phi_2 - \eta_2$
	CH bend (out-of-plane)	$S_{23} = \mu_1 - \mu_2$
	CH_2 wag	$S_{24} = \alpha_1 - \beta_1 + \phi_1 - \eta_1 - \alpha_2 + \beta_2 - \phi_2 + \eta_2$
	ring deformation	$S_{25} = R_2 - R_3$
	CH_2 rock	$S_{26} = \alpha_1 + \beta_1 - \phi_1 - \eta_1 - \alpha_2 - \beta_2 + \phi_2 + \eta_2$
	SiH_2 twist	$S_{27} = \pi_1 - \pi_2 - \sigma_1 + \sigma_2$
	SiH_2 rock	$S_{28} = \pi_1 - \pi_2 + \sigma_1 - \sigma_2$
	ring−Si bend (out-of-plane)	$S_{29} = \epsilon_1 - \epsilon_2$
	$SiClH_2$ torsion	$S_{30} = \tau$

[a] Not normalized.

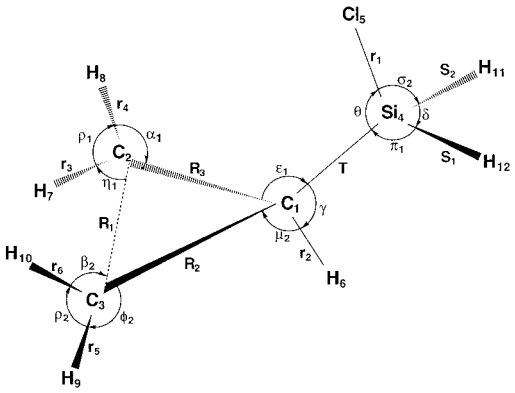

Figure 5. Internal coordinates of cyclopropylchlorosilane.

The ring breathing fundamental is easily recognizable by its strength and polarization in the Raman spectrum of the liquid at 1189 cm^{-1}. The other two ring deformational modes are located at 900 and 834 cm^{-1} in the infrared spectrum of the solid for the gauche conformer. For the cis conformer, the A″ ring deformation is expected to appear approximately 40 cm^{-1} above the 834 cm^{-1} band assigned to the gauche form. However, it is masked by another gauche fundamental, the SiH_2 waging motion, which gives rise to the very strong infrared absorption at 873 cm^{-1} in the spectra of the xenon solutions. The corresponding SiH_2 wag of the cis form is well resolved and appears at 854 cm^{-1} in the same spectrum. Another well-resolved conformer doublet in the spectrum of the xenon solution is due to the SiH_2 deformations of the cis and gauche conformers at 956 and 943 cm^{-1}, respectively. The A-type Q-branches located at 721 and 578 cm^{-1} in the infrared spectrum of the gas are assigned to the SiH_2 twist and rock of the gauche conformer, whereas the depolarized Raman band at 697 cm^{-1} (liquid) and the C-type Q-branch at 610 cm^{-1} (gas) are attributed to the respective modes of the cis form.

The C−Si stretching conformer pair is observed in the Raman spectrum of the liquid at 668 and 628 cm^{-1} for the gauche and cis conformer, respectively. Only the former band is seen in the spectrum of the crystalline solid. A series of bands with maxima at 531, 525, 519, and 513 cm^{-1} in the spectrum of the sample dissolved in liquid xenon are associated with the Si−Cl stretching fundamental (Figure 3A). Considering the isotopic shift factors, the former two bands are assigned to the Si−Cl stretches of the ^{35}Cl and ^{37}Cl isotopes of the gauche conformer, whereas the latter two are the equivalent modes for the cis form. The in-plane and out-of-plane ring−Si bends of the gauche conformer are observed as weak polarized bands at 239 and 289 cm^{-1} in the Raman spectrum of the liquid which remain in the spectrum of the solid (Figure 1). The in-plane vibration of the cis form produces the prominent Q-branch at 349 cm^{-1} in the far-infrared spectrum of the gas which is also evident in the far-infrared spectrum of the amorphous solid but disappears upon annealing (Figure 4). As anticipated from the *ab initio* prediction of zero infrared and Raman spectral intensities for the A″ ring−Si bend of the cis form which is expected at about 215 cm^{-1}, this mode is not observed in either spectra. The B-type band located at 124 cm^{-1} in the far-infrared spectrum of the gas is associated with the CSiCl bending, and the weak absorption centered at ∼60 cm^{-1} with a series of Q-branches is assigned to the asymmetric torsion of both conformers with the higher frequency absorption attributed to the cis rotamer.

Discussion

The structural parameters listed in Table 2 are fairly consistent among the six basis sets utilized with the major exceptions occurring with the two heavy atom parameters. The C−Si bond distance is approximately 0.005 Å shorter for the gauche conformer with all basis sets. The ClSiC bond angle is approximately 2.5° smaller for the cis conformer than the gauche conformer again for all basis sets. Additionally, a comparison

TABLE 4: Comparison of Observed and Calculated Frequencies (cm^{-1}) for Cyclopropylchlorosilane

			cis							gauche						
	vib no.	fundamental	*ab*[a] *initio*	fixed[b] scaled	IR[c] int	Raman act[d]	dp[d] ratio	obs.[e]	PED[f]	*ab*[a] *initio*	fixed[b] scaled	IR[c] int	Raman act.[d]	dp[d] ratio	obs[e]	PED[f]
A′	ν_1	CH_2 antisymmetric stretch	3307	3137	7.5	42.2	0.61	3091	$100S_1$	3301	3132	8.6	54.5	0.51	3091	$99S_1$
	ν_2	CH_2 symmetric stretch	3212	3047	4.8	176.2	0.05	3014	$96S_2$	3206	3042	6.8	189.3	0.10	(3007)	$97S_2$
	ν_3	CH stretch	3197	3032	3.5	77.4	0.46	3014	$96S_3$	3220	3055	0.5	37.5	0.36	(3014)	$97S_3$
	ν_4	SiH_2 symmetric stretch	2321	2202	148.3	184.8	0.06	2186	$100S_4$	2318	2199	108.6	43.7	0.15	2185	$96S_4$
	ν_5	CH_2 deformation	1569	1488	0.2	4.6	0.66	1457	$89S_5$, $10S_7$	1571	1490	1.6	4.4	0.68	1457	$90S_5$
	ν_6	CH bend (in-plane)	1371	1301	17.0	4.2	0.53	1293	$45S_6$, $25S_7$, $12S_9$	1371	1300	22.5	4.9	0.56	1292	$46S_6$, $23S_7$, $12S_9$
	ν_7	ring breathing	1265	1200	4.6	24.8	0.12	1190	$58S_7$, $12S_9$	1263	1198	4.6	26.5	0.10	1186	$60S_7$, $17S_6$, $11S_9$
	ν_8	CH_2 wag	1120	1063	13.2	1.2	0.14	1045	$88S_8$	1118	1061	10.9	2.2	0.20	1045	$73S_8$
	ν_9	CH_2 twist	1084	1028	31.5	7.7	0.70	1022	$26S_9$, $27S_6$, $26S_{13}$	1085	1029	5.7	4.6	0.72	1022	$23S_9$, $26S_6$, $23S_{12}$
	ν_{10}	SiH_2 deformation	1009	957	107.8	14.8	0.71	960	$94S_{10}$	994	943	128.4	14.2	0.75	946	$95S_{10}$
	ν_{11}	ring deformation	974	924	89.6	16.9	0.72	906	$79S_{11}$, $10S_{14}$	970	920	51.4	8.8	0.73	(899)	$80S_{11}$
	ν_{12}	SiH_2 wag	900	853	277.5	11.0	0.70	860	$79S_{12}$, $14S_{13}$	936	888	224.8	11.9	0.74	879	$54S_{12}$, $28S_{25}$
	ν_{13}	CH_2 rock	826	783	12.2	0.1	0.71	788	$50S_{13}$, $41S_9$	836	794	5.6	2.2	0.71	798	$62S_{13}$, $28S_9$
	ν_{14}	CSi stretch	650	617	16.6	12.3	0.54	(626)	$57S_{14}$, $12S_{15}$, $10S_{11}$	697	661	30.2	7.7	0.48	669	$41S_{14}$, $24S_{28}$, $10S_{27}$
	ν_{15}	SiCl stretch	543	516	49.6	9.6	0.13	(519)	$84S_{15}$, $12S_{14}$	557	528	69.3	8.5	0.22	531	$79S_{15}$
	ν_{16}	ring−Si bend (in-plane)	363	345	6.8	2.5	0.61	349	$57S_{16}$, $30S_{17}$	244	231	0.9	0.8	0.05	235	$81S_{16}$
	ν_{17}	CSiCl bend	135	128	1.5	1.0	0.66	124	$65S_{17}$, $33S_{16}$	126	121	1.6	0.9	0.71	124	$54S_{17}$, $30S_{29}$, $13S_{30}$
A″	ν_{18}	CH_2 antisymmetric stretch	3296	3127	0.3	83.9	0.75	3089	$100S_{18}$	3290	3121	0.1	90.7	0.75	3089	$99S_{18}$
	ν_{19}	CH_2 symmetric stretch	3208	3043	8.2	28.6	0.75	3009	$100S_{19}$	3202	3038	9.1	31.4	0.60	(3000)	$99S_{19}$
	ν_{20}	SiH_2 antisymmetric stretch	2329	2209	164.5	75.7	0.75	2189	$100S_{20}$	2331	2211	162.1	123.3	0.22	2189	$96S_{20}$
	ν_{21}	CH_2 deformation	1532	1453	3.2	8.3	0.75	(1430)	$100S_{21}$	1535	1456	2.4	9.1	0.75	1436	$100S_{21}$
	ν_{22}	CH_2 twist	1242	1178	0.5	6.2	0.75	1178	$43S_{22}$, $48S_{26}$	1240	1176	0.3	5.6	0.72	1178	$40S_{22}$, $49S_{26}$, $10S_{23}$
	ν_{23}	CH bend (out-of-plane)	1172	1111	4.8	0.8	0.75	1095	$52S_{23}$, $36S_{22}$	1175	1114	4.3	0.7	0.71	1096	$53S_{23}$, $38S_{22}$
	ν_{24}	CH_2 wag	1127	1069	2.4	0.2	0.75	1068	$95S_{24}$	1125	1067	5.0	0.2	0.68	1064	$90S_{24}$
	ν_{25}	ring deformation	934	886	3.2	10.0	0.75	879	$74S_{25}$	896	850	116.4	22.6	0.72	840	$65S_{25}$, $34S_{12}$
	ν_{26}	CH_2 rock	871	827	16.4	7.0	0.75	829	$31S_{26}$, $28S_{23}$, $22S_{25}$, $14S_{22}$	865	822	21.2	2.8	0.73	824	$35S_{26}$, $26S_{23}$, $16S_{22}$, $11S_{25}$
	ν_{27}	SiH_2 twist	712	675	0.3	16.2	0.75	(698)	$89S_{27}$	753	714	8.6	13.9	0.75	721	$75S_{27}$, $10S_9$
	ν_{28}	SiH_2 rock	633	601	50.3	3.9	0.75	610	$89S_{28}$	597	566	41.5	6.8	0.54	578	$60S_{28}$, $14S_{14}$, $12S_{15}$
	ν_{29}	ring−Si bend (out-of-plane)	228	217	0.0	0.0	0.75		$89S_{29}$	295	280	3.4	3.4	0.52	283	$48S_{29}$, $34S_{17}$
	ν_{30}	$SiClH_2$ torsion	78	78	0.1	0.2	0.75	68	$98S_{30}$	67	66	0.5	0.3	0.71	57	$82S_{30}$, $12S_{29}$

[a] Calculated with the MP2/6-31G* basis set. [b] Scaling factors of 0.9 for stretching and bending coordinates and 1.0 for torsional coordinates. [c] Calculated infrared intensities in km/mol. [d] Calculated Raman activities in $Å^4$/amu, using RHF/6-31G* basis set. [e] Frequencies are taken from the infrared spectrum of the gas, except the ones in parentheses which are taken from the infrared spectrum of the xenon solution or the solid. [f] For a description of the symmetric coordinates see Table 3.

TABLE 5: Temperature and Intensity Ratios for the Conformational Study of Cyclopropylchlorosilane in Liquid Xenon

T (°C)	T (K)	1000/T (K)	I_{956}/I_{943}	−ln K	I_{787}/I_{796}	−ln K	I_{626}/I_{667}	−ln K	I_{608}/I_{577}	−ln K
−55	218	4.587	0.340	1.078	0.403	0.908	0.782	0.246	0.694	0.367
−60	213	4.695	0.349	1.054	0.452	0.793	0.695	0.363	0.629	0.464
−65	208	4.808	0.360	1.021	0.459	0.780	0.763	0.270	0.692	0.368
−70	203	4.926	0.365	1.009	0.486	0.722	0.750	0.288	0.693	0.367
−75	198	5.051	0.371	0.991	0.485	0.724	0.762	0.272	0.722	0.326
−80	193	5.181	0.374	0.982	0.466	0.763	0.799	0.225	0.738	0.304
−85	188	5.319	0.381	0.966	0.485	0.244	0.812	0.209	0.749	0.289
−90	183	5.464	0.387	0.949	0.506	0.681	0.849	0.163	0.781	0.247
−95	178	5.618	0.385	0.955	0.507	0.679	0.809	0.212	0.740	0.302
−100	173	5.780	0.396	0.927	0.504	0.685	0.912	0.093	0.804	0.218
ΔH^a (cm^{-1})				80 ± 8		102 ± 24		106 ± 25		106 ± 21

[a] Average $\Delta H = 98 \pm 10$ cm^{-1} (281 ± 29 cal/mol), with the cis conformer more stable.

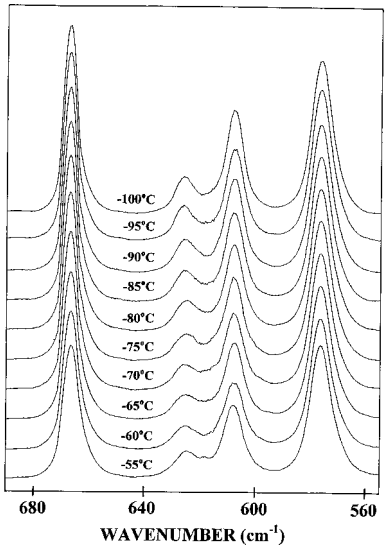

Figure 6. Temperature-dependent infrared spectrum of cyclopropylchlorosilane.

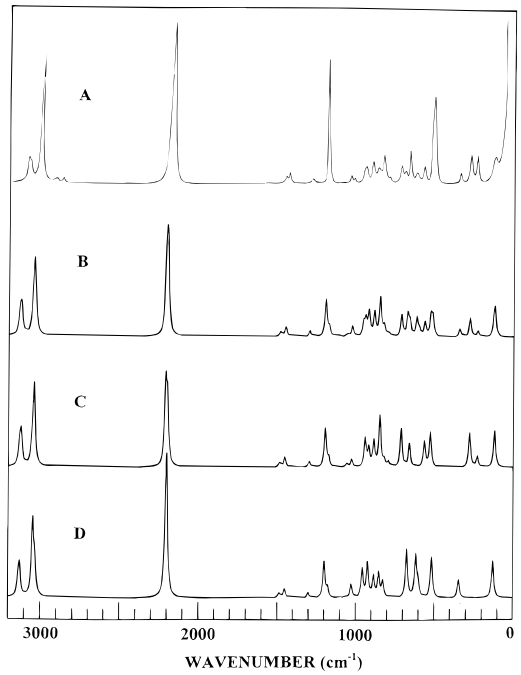

Figure 7. Raman spectra of cyclopropylchlorosilane: (A) experimental spectrum of the liquid; (B) calculated spectrum of the mixture of both conformers; (C) calculated spectrum of the gauche conformer; and (D) calculated spectrum of the cis conformer.

of the structural parameters obtained for cyclopropylchlorosilane with those previously reported for cyclopropyldichlorosilane[20] reveals some interesting differences. First, when considering the values obtained from the MP2/6-311+G** basis set for the C−Si bond distance, a comparison between these two molecules shows that the value obtained for the monochlorosubstituted silane is approximately 0.014 Å longer than the similar bond of the corresponding dichlorosilane. Also utilizing the same basis set, the values obtained for the Si−Cl and Si−H bond distances are roughly 0.018 and 0.006 Å shorter than the corresponding bond for the dichloro compound. At the RHF level both the C−Si and Si−Cl bond distances are predicted to be considerably longer (∼0.010 Å) than the values obtained from the MP2 calculations. Additionally, all basis sets with a triple-split valence shell tend to yield longer C−Si and shorter C−C bond distances.

Raman and infrared spectra (Figures 7 and 3) for cyclopropylchlorosilane were calculated using the frequencies, scattering activities and intensities determined from the MP2/6-31G* calculations. The Gaussian-92 program[18] with the option of calculating the polarizability derivatives was used. The Raman scattering cross sections, $\partial\sigma_j/\partial\Omega$, which are proportional to the Raman intensities, can be calculated from the scattering activities and the predicted frequencies for each normal mode using the relationship[25]

$$\frac{\partial\sigma_j}{\partial\Omega} = \left(\frac{2^4\pi^4}{45}\right)\left(\frac{(\nu_0 - \nu_j)^4}{1 - \exp\left[\frac{-hc\nu_j}{kT}\right]}\right)\left(\frac{h}{8\pi^2 c\nu_j}\right)S_j$$

where ν_0 is the exciting frequency, ν_j is the vibrational frequency of the jth normal mode, h, c, and k are universal constants, and S_j is the corresponding Raman scattering activity. To obtain the polarized Raman scattering cross section, the polarizabilities are incorporated into S_j by $S_j[(1 - r_j)/(1 + r_j)]$, where r_j is the depolarization ratio of the jth normal mode. The Raman scattering cross sections and calculated frequencies are used together with a Lorentzian line-shape function to obtain the calculated spectrum. Since the calculated frequencies are ≈10% higher than those observed, the frequency axis of the theoretical spectrum was compressed by a factor of 0.9. The predicted Raman spectra of the gauche and cis pure conformers are shown in Figure 7 C and D, respectively. The predicted Raman spectrum of the mixture of the two conformers with an assumed ΔH of 98 cm^{-1} is shown in Figure 7B. This spectrum should be compared to the experimental spectrum of the liquid (Figure 7A). The calculated Raman spectrum is quite similar to the experimental spectrum with the exception of the intensities of the ring-breathing and SiCl stretching fundamentals which are predicted too weak. The same problem was encountered in the calculated spectrum of cyclopropyldichlorosilane,[20] where the ring-breathing and $SiCl_2$ symmetric stretch were also predicted too weak compared to the experimental intensities. Another discrepancy between the observed and calculated spectra is in

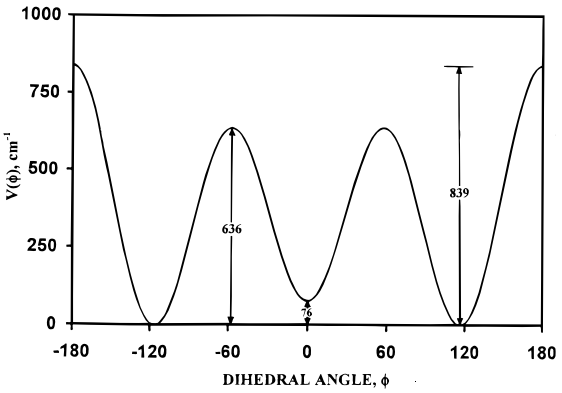

Figure 8. Potential function of the asymmetric torsion of cyclopropylchlorosilane as calculated with the MP2/6-31G* basis set. A dihedral angle of 0° corresponds to the cis conformer.

the relative intensities of the conformer band pairs, where the bands of the cis conformer are calculated a little too strong. This is probably due to the use in the calculation of a ΔH value representative for the gas phase rather than the neat liquid. A smaller ΔH in the liquid phase would lead to a reduction of the band intensities for the cis conformer. Actually, the calculated dipole moment of the gauche conformer is larger than that of the cis (Table 2), which should stabilize the gauche form in the condensed phases. This factor, coupled with other packing interactions, is probably the reason the gauche conformer is more stable in the solid, whereas the cis form is more stable in the gas.

Infrared intensities were also calculated based on the dipole moment derivatives with respect to the Cartesian coordinates. The derivatives were taken from the *ab initio* calculations and transformed to normal coordinates by

$$\left(\frac{\partial \mu_\mu}{\partial Q_i}\right) = \sum_j \left(\frac{\partial \mu_\mu}{\partial X_j}\right) L_{ji}$$

where the Q_i is the ith normal coordinates, X_j is the jth Cartesian displacement coordinates, and L_{ji} is the transformation matrix between the Cartesian displacement coordinates and normal coordinates. The infrared intensities were then calculated by

$$I_i = \frac{N\pi}{3c^2}\left[\left(\frac{\partial \mu_x}{\partial Q_i}\right)^2 + \left(\frac{\partial \mu_y}{\partial Q_i}\right)^2 + \left(\frac{\partial \mu_z}{\partial Q_i}\right)^2\right]$$

In Figure 3, C and D, the predicted infrared spectra of the two conformers are shown. The combination of the spectra of the two conformers with a ΔH of 98 cm^{-1} is shown in Figure 3B. The experimental infrared spectrum of the sample dissolved in liquid xenon at −70 °C is also shown for comparison. Excluding the overtones, combination bands and several impurity bands which are present in the spectrum of the xenon solution, the agreement between the observed and calculated spectra is satisfactory and it provides support for the vibrational assignments.

The potential surface (Figure 8) of the asymmetric torsion was obtained by relaxation of all structural parameters in the expected potential minima and maxima using the MP2/6-31G* basis set. Since the calculated energy difference of 76 cm^{-1} from the MP2/6-31G* calculation with the gauche conformer more stable contradicts the experimental results from the variable-temperature study, the relative energies of the potential wells are obviously inaccurate. Nevertheless, the barriers to internal rotation are compatible to those calculated for cyclopropyldichlorosilane;[20] however, the gauche-to-cis barrier in cyclopropylchlorosilane is about 200 cm^{-1} lower than the gauche-to-gauche barrier which contrasts that in the dichloro compound where the two barriers have almost the same magnitude (~710 cm^{-1}).

The vibrational modes of c-$C_3H_5SiH_2Cl$ are relatively pure as can be seen from the PED in Table 4. The exceptions are in the CH_2 twist, CH_2 rock, and the CH bending modes which are extensively mixed in the fundamentals at 1293, 1178, 1095, 1022, and 788 cm^{-1}. The frequency predictions from the MP2/6-31G* calculations are quite good and very helpful in the vibrational assignment. Slight variations in the predicted frequencies of the ring deformations (ν_{25}', ν_{11}, and ν_{11}') create the minor mismatch between the observed and calculated infrared spectra in the 1000−800 cm^{-1} region (Figure 3).

It is quite surprising that even at relatively high levels of calculations the *ab initio* results fail to predict the more stable conformer of cyclopropylchlorosilane. Only the MP2/6-311++G** basis set favors the cis conformer as more stable. Since such a wide variety of basis sets were utilized to calculate the structure and conformational energy, it is possible to draw some conclusions for the applicability of these basis sets to predicting similar conformational equilibria. By examining the trends in the conformational energy differences, ΔE, given in Table 2, one can conclude that the use of "triple-split valence" (6-311) basis sets by itself does not greatly improve the ΔE prediction. Conversely, the addition of diffuse orbitals, especially to the heavy atoms (6-31+), proves to be more significant in the calculations. For example, a comparison of the 6-311G** ($\Delta E = 56$ cm^{-1}) versus the 6-31++G** ($\Delta E = 23$ cm^{-1}) basis sets, shows that the latter is closer to predicting the more stable conformer. Also, the addition of a (+) to the 6-311G** basis set improves the prediction to $\Delta E = 9$ cm^{-1}. Finally, the largest basis set 6-311++G** gives the proper conformational stability. It is believed that the diffuse orbitals help in the modeling of the size of the Cl-atom orbitals and thus the intramolecular interaction between the Cl atom and the ring which may be the reason for the stabilization of the cis conformer.

It is difficult to ascertain how well the *ab initio* calculations predict the structural parameters since there is very limited data on C−Si and Si−Cl distances for similar molecules. For example, microwave data are available for vinylchlorosilane but no data were obtained for the isotopic carbon atoms.[26,27] Comparing the calculated C−Si and Si−Cl distances from the RHF/6-31G* calculations for vinylchlorosilane with the corresponding distances for cyclopropylchlorosilane indicates that the C−Si should be shorter by about 0.006 Å for the three-membered ring molecule whereas the Si−Cl distance should be longer by the same amount for the cis conformers. However, for the gauche conformer the Si−Cl distances are predicted to be about the same for these two molecules but the C−Si distances are predicted to have about the same difference as for the cis rotamers. Electron diffraction studies of these two molecules using the proposed differences for the C−Si and Si−Cl parameters for the two conformers as constraints should provide reliable structural parameters. Such parameters could then be used to provide offset values for the *ab initio* calculations which then could be used for accurate predictions for other silicon−chlorine containing molecules.

Acknowledgment. J.R.D. acknowledges partial support of these studies by the University of Missouri−Kansas City Faculty Research Grant program.

References and Notes

(1) Saebo, S.; Kavana, K. *J. Mol. Struct.* **1991**, *235*, 447.

(2) Fujiwara, F. G.; Chang, J. C.; Kim, H. *J. Mol. Spectrosc*. **1977**, *41*, 177.
(3) Mohammadi, M. A.; Brooks, W. V. F. *J. Mol. Spectrosc.* **1978**, *73*, 347.
(4) Mohammadi, M. A.; Brooks, W. V. F. *Can. J. Spectrosc*. **1978**, *23*, 181.
(5) Schei, S. H. *Acta Chem. Scand., Ser. A* **1983**, *37*, 15.
(6) Durig, J. R.; Godbey, S. E.; Faust, S. A. *J. Mol. Struct*. **1988**, *176*, 123.
(7) Kalasinsky, V. F.; Wurrey, C. J. *J. Raman Spectrosc.* **1980**, *9*, 315.
(8) Wurrey, C. J.; Krishnamoorthi, R.; Pechsiri, S.; Kalasinsky, V. F. *J. Raman Spectrosc*. **1982**, *12*, 95.
(9) Wurrey, C. J.; Yeh, Y. Y.; Weakley, M. D.; Kalasinsky, V. F. *J. Raman Spectrosc*. **1984**, *15*, 179.
(10) Wurrey, C. J.; DeWitt, J. E.; Kalasinsky, V. F. In *Vibrational Spectra and Conformational Analysis of Substituted Three Membered Ring Compounds*; Durig, J. R., Ed.; Elsevier: Amsterdam, 1983; Vol. 12, Chapter 4.
(11) Stolevik, R.; Bakken, P. *J. Mol. Struct*. **1989**, *196*, 285.
(12) Dakkouri, M.; Grunvogel-Hurst, A., to be published.
(13) Little, T. S.; Qtaitat, M.; Durig, J. R.; Dakkouri, M.; Dakkouri, A. *J. Raman Spectrosc*. **1990**, *21*, 591.
(14) Simons, H. E.; Smith, R. D. *J. Am. Chem. Soc*. **1959**, *81*, 4256.
(15) Dakkouri, M.; Kehrer, H.; Buhmann, P. *Chem. Ber*. **1979**, *112*, 3523.
(16) Furic, K.; Durig, J. R. *Appl. Spectrosc*. **1988**, *42*, 175.
(17) Miller, F. A.; Harney, B. M. *Appl. Spectrosc*. **1970**, *24*, 291.
(18) *Gaussian-92*, Revision C.4; Frisch, M. J.; Trucks, G. W.; Head-Gordon, M.; Gill, P. M. W.; Wong, M. W.; Foresman, J. B.; Johnson, B. J.; Schlegel, H. B.; Robb, M. A.; Replogle, E. S.; Gomperts, R.; Andres, J. L.; Raghavachari, K.; Binkley, J. S.; Gonzalez, C.; Martin, R. L.; Fox, D. J.; DeFrees, D. J.; Baker, J.; Stewart, J. J. P.; Pople, J. A. Gaussian, Inc.: Pittsburgh, PA, 1992.
(19) Pulay, P. *Mol. Phys*. **1969**, *17*, 197.
(20) Durig, J. R.; Hur, Seung Won; Dakkouri, M.; Grunvogel-Hurst, A.; Gounev, T. K. *Chem. Phys*., submitted for publication.
(21) Schachtschneider, J. H. *Vibrational Analysis of Polyatomic Molecules*; Parts V and VI, Technical Report Nos. 231 and 57; Shell Development Co.: Houston, TX, 1964, 1965.
(22) Herrebout, W. A.; van der Veken, B. J.; Wang, Aiying; Durig, J. R. *J. Phys. Chem.* **1995**, *99*, 578.
(23) Herrebout, W. A.; van der Veken, B. J. *J. Phys. Chem*. **1996**, *100*, 9671.
(24) van der Veken, B. J. *J. Phys. Chem*. **1996**, *100*, 17436.
(25) Chantry, G. W. In *The Raman Effect*; Anderson, A., Ed.; Marcel Dekker: Inc.: New York, 1971; Vol. 1, Chapter 2.
(26) Imachi, M. *J. Sci. Hiroshima University Ser. A* **1978**, *42*, 43.
(27) Sullivan, J. F.; Qtaitat, M. A.; Durig, J. R. *J. Mol. Struct. (THEOCHEM)* **1989**, *202*, 159.